Available online at www.sciencedirect.com
SCIENCE DIRECT®
Journal of Sound and Vibration 292 (2006) 661–675
JOURNAL OF SOUND AND VIBRATION
www.elsevier.com/locate/jsvi

The generalized Vincent circle in vibration suppression

Maryam Ghandchi Tehrani[a], Weizhuo Wang[a], Cristinel Mares[b], John E. Mottershead[a,*]

[a]*Mechanical Engineering Division, Department of Engineering, The University of Liverpool, Liverpool L69 3GH, UK*
[b]*School of Engineering and Design, Brunel University, Uxbridge, Middlesex UB8 3PH, UK*

Received 17 August 2004; received in revised form 15 August 2005; accepted 23 August 2005
Available online 7 November 2005

Abstract

In 1972 A. H. Vincent, the then Chief Dynamicist at Westland Helicopters, discovered that when a structure excited at point p with a constant frequency is modified, for example by the addition of a spring between two points r and s, then the response at another point q traces a circle when plotted in the complex plane as the spring stiffness is varied from minus infinity to plus infinity. This discovery, although apparently little known today, has many useful applications some of which are described in papers by various authors appearing in the 1970s and early 1980s. Vincent's discovery is in fact a particular example of the bilinear transformation due to August Ferdinand Moebius (1790–1868). In this paper, the Vincent circle method is generalized for the case of any straight-line modification in the complex plane, typically $z = k + \mathrm{i}\omega c - \omega^2 m$, where $c = \alpha(k - \omega^2 m) + \beta$. A new method for the visualization of Vincent circle results, including the case of multiple modifications is also presented.

1. Introduction

Predicting the effect of a local modification, such as an added stiffness, mass or viscous damper, on the vibration characteristics of an elasto-mechanical system is a frequently encountered problem. Vincent [1] observed that when a structure excited at a point q with a constant frequency was modified, for example by the addition of a spring between two coordinates r and s, then the response at another point p traced out a circle when plotted in the complex plane as the spring stiffness was varied between minus and plus infinity. Vincent's circle is in fact a particular manifestation of the Moebius' transformation [2], which maps straight lines and circles in one complex domain onto straight lines and circles in another. In the structural modification problem, the modification itself can the expressed as a complex dynamic stiffness, typically of the form $k_{rs} + \mathrm{i}\omega c_{rs}$, between r and s. Apparently Vincent, and other authors [3–5] writing at the same time, were unaware of the Moebius transformation because they restricted their attention to only one straight line—the stiffness modification line—along the real axis of the complex modification plane. When a viscous damping coefficient is varied between plus and minus infinity along the imaginary axis, a Vincent circle will also be

*Corresponding author. Tel.: +44 151 794 4827; fax: +44 151 794 4848.
E-mail address: j.e.mottershead@liv.ac.uk (J.E. Mottershead).

0022-460X/$ - see front matter © 2005 Elsevier Ltd. All rights reserved.
doi:10.1016/j.jsv.2005.08.024

Nomenclature

$\mathbf{C}$	viscous damping matrix
$\mathbf{H}(\omega)$	receptance matrix
$\overline{\mathbf{H}}(\omega)$	modified receptance matrix
$\mathbf{e}_p, \mathbf{e}_q, \mathbf{e}_r, \mathbf{e}_s$	unit vectors formed from the pth, qth, rth and sth column of the identity matrix, respectively
$\mathbf{K}$	stiffness matrix
$\mathbf{M}$	mass matrix
a, b, c, d	Vincent circle parameters
c, k, m	modification parameters
C0, C1, C2	circle names
$h_{pq}(\omega)$	pqth term of the receptance matrix
$\bar{h}_{pq}(\omega)$	pqth term of the modified receptance matrix
p, q, r, s	coordinates
$z_{rs}(\omega)$	dynamic stiffness of modification between two coordinates r and s
z_1, z_2	variable parameters
$\Delta k^*, \Delta m^*, \Delta z^*$	modification parameters
$\Delta z_1, \Delta z_2$	increment of z_1 and z_2
α, β	coefficients of the straight line
$\alpha, \beta, \gamma, \delta$	Moebius transformation coefficients
ξ	centre of Vincent's circle
ρ	radius of Vincent's circle
ω	radian frequency

traced in the plane of a complex receptance, as will a general straight-line modification of the form $c_{rs} = \alpha k_{rs} + \beta$, $-\infty > k_{rs} > \infty$.

The assignment of natural frequencies and antiresonances [6] is an important aspect of vibration suppression and the closest point on the Vincent circle to the origin of the complex receptance plane defines the parameter that reduces the vibration response to a minimum at the chosen frequency. A closed-form solution of the vibration reduction problem using Vincent's circle was presented by Mottershead and Ram [7]. In this paper, the theory of Vincent's circle is described and a new technique for the visualization of results explained. Numerical and experimental example problems are discussed.

2. Theory

In the general case of a modification $z_{rs}(\omega) = k_{rs} + \omega c_{rs}$ connected between the rth and sth coordinates the matrix of receptances may be expressed as

$$\overline{\mathbf{H}}(\omega) = \left(\mathbf{K} + \omega\mathbf{C} - \omega^2\mathbf{M} + z_{rs}(\omega)(\mathbf{e}_r - \mathbf{e}_s)(\mathbf{e}_r - \mathbf{e}_s)^{\mathrm{T}}\right)^{-1}, \tag{1}$$

where the overbar denotes the modified system. e_r is the unit vector formed from the rth column of the identity matrix. A list of symbols is given in Nomenclature.

Application of the Sherman–Morrison formula [8] leads to an expression for the modified-system receptances in terms of the receptances of the original system

$$\overline{\mathbf{H}}(\omega) = \mathbf{H}(\omega) - \frac{z_{rs}(\omega)\mathbf{H}(\omega)(\mathbf{e}_r - \mathbf{e}_s)(\mathbf{e}_r - \mathbf{e}_s)^{\mathrm{T}}\mathbf{H}(\omega)}{1 + z_{rs}(\omega)(\mathbf{e}_r - \mathbf{e}_s)^{\mathrm{T}}\mathbf{H}(\omega)(\mathbf{e}_r - \mathbf{e}_s)}. \tag{2}$$

The pqth term can then be selected from the matrix of modified receptances by

$$\overline{h}_{pq} = \mathbf{e}_p^{\mathrm{T}}\hat{\mathbf{H}}(\omega)\mathbf{e}_q, \tag{3}$$

which may be written explicitly in the form

$$\bar{h}_{pq}(\omega) = h_{pq}(\omega) - \frac{z_{rs}(\omega)(h_{pr}(\omega) - h_{ps}(\omega))(h_{rq}(\omega) - h_{sq}(\omega))}{1 + z_{rs}(\omega)(h_{rr}(\omega) - h_{rs}(\omega) - h_{sr}(\omega) + h_{ss}(\omega))}, \tag{4}$$

where $h_{pq}(\omega)$, $h_{pr}(\omega)$, $h_{ps}(\omega)$, $h_{rq}(\omega)$, $h_{sq}(\omega)$, $h_{rr}(\omega)$, $h_{rs}(\omega)$, $h_{sr}(\omega)$, $h_{ss}(\omega)$ are receptances of the original system and $\bar{h}_{pq}(\omega)$ is the desired receptance of the modified system.

Eq. (4) represents the most general case but may be straightforwardly simplified for the cases of (i) a point receptance ($p = q$)

$$\bar{h}_{qq}(\omega) = h_{qq}(\omega) - \frac{z_{rs}(\omega)(h_{qr}(\omega) - h_{qs}(\omega))^2}{1 + z_{rs}(\omega)(h_{rr}(\omega) - h_{rs}(\omega) - h_{sr}(\omega) + h_{ss}(\omega))}. \tag{5}$$

(ii) Co-incidence of a receptance and a modification coordinate ($p = r$)

$$\bar{h}_{rq}(\omega) = h_{rq}(\omega) - \frac{z_{rs}(\omega)\big(h_{rr}(\omega) - h_{rs}(\omega))(h_{rq}(\omega) - h_{sq}(\omega)\big)}{1 + z_{rs}(\omega)(h_{rr}(\omega) - h_{rs}(\omega) - h_{sr}(\omega) + h_{ss}(\omega))} \tag{6}$$

and (iii) point modifications $\big(z_{rs}(\omega) = z_{rr}(\omega),\ h_{ps}(\omega) = h_{sq}(\omega) = h_{rs}(\omega) = h_{sr}(\omega) = h_{ss}(\omega) = 0\big)$, which might include a point mass, so that $z_{rr}(\omega) = k_{rr} + \mathrm{i}\omega c_{rr} - \omega^2 m_{rr}$,

$$\bar{h}_{pq}(\omega) = \frac{h_{pq}(\omega) + z_{rr}(\omega)\big(h_{pq}(\omega)h_{rr}(\omega) - h_{pr}(\omega)h_{rq}(\omega)\big)}{1 + z_{rr}(\omega)h_{rr}(\omega)}. \tag{7}$$

2.1. Vincent's circle—the case of a general straight-line modification

Vincent's circle is best explained when Eq. (4) is written in the simplified form [7]

$$a = b + \frac{zc}{1 + zd}, \quad a = \bar{h}_{pq}(\omega), \quad a, b, c, d \in C, \tag{8}$$

where C denotes the set of complex numbers.

The more general Moebius transformation [2], which provides a one-to-one conformal mapping of the z-plane to the Z-plane, is generally written as

$$Z = \frac{\alpha z + \beta}{\gamma z + \delta}, \quad \alpha\delta - \beta\gamma \neq 0, \tag{9}$$

where in this particular case

$$Z = a, \quad \alpha = bd + c, \quad \beta = b, \quad \delta = 1, \quad \gamma = d. \tag{10}$$

The Moebius transformation is sometimes called the bilinear transformation because it is derived from the bilinear relation between two variables z and Z

$$\gamma z Z + \delta Z - \alpha z - \beta = 0. \tag{11}$$

The property which explains why the response Z can be represented as a circle at a fixed frequency as a function of the structural modification $z \in C$, is that every Mobius transformation (8), (9) maps circles into circles, real circles (including straight lines) into real circles or straight lines and imaginary circles into imaginary circles. Details can be found in Chapter 6 of Ref. [2].

Done and Hughes [3] showed that the imaginary part of z is zero if and only if a is on the perimeter of a circle, the radius and centre of which may be expressed as

$$\rho = \left|\frac{c}{2\,\mathrm{imag}(d)}\right|, \quad \xi = b - \frac{\mathrm{i}c\rho}{|c|} \tag{12), (13}$$

which is of course the case of a strictly real modification ($z = k - \omega^2 m$).

Similar analysis in the case of a purely imaginary modification [8], the Vincent circle of a viscous damper, shows that

$$\rho = \left|\frac{c}{2\,\mathrm{real}(d)}\right|, \quad \xi = b + \frac{c\rho}{|c|}. \tag{14), (15}$$

And for a complex modification, $z = k + \mathrm{i}\omega c - \omega^2 m$, of the form $c = \alpha(k - \omega^2 m) + \beta$

$$\rho = \left|\sqrt{\frac{\beta\omega c c^*}{A} + BB^*}\right|, \quad \xi = b + B, \tag{16), (17}$$

$$A = \text{imag}(d) + \alpha\omega\,\text{real}(d) - \beta\omega dd^*, \quad B = \frac{(\omega(\alpha - 2\beta d^*) - \text{i})c}{2A}, \tag{18), (19}$$

where $(\cdot)^*$ denotes the complex conjugate. The derivation of Eqs. (16) and (17) is given in Appendix A.

The point on the circle closest to the origin of the complex plane corresponds to the greatest possible suppression of vibration as shown in Fig. 1. The strictly real modification k resulting in the minimum of $|a|$ was determined in closed form by Mottershead and Ram [7]. Similar closed-form solutions are of course available for the purely imaginary modification and general straight-line modification $c = \alpha(k - \omega^2 m) + \beta$.

2.2. Visualization of Vincent circle results

Consider an arbitrary multi-degree-of-freedom system. In order to study the effect of a structural modification over a range of frequencies the modified receptance a represented by distinct circles at each frequency increment, when $z \in C$, may be laid on top of each other to form a 3D surface where the vertical axis represents frequency and the circles are in the horizontal plane, as shown in Fig. 2. The surface represents an envelope of the Vincent circles and the 3D curve revolving around the surface represents the receptances at all frequencies when the modification is zero. The projection of this curve on the zero frequency plane represents the polar diagram of the system. The 3D plot was described previously [3] and is only included so that the account presented here is complete.

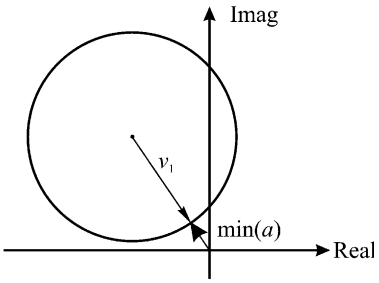

Fig. 1. Vincent's circle.

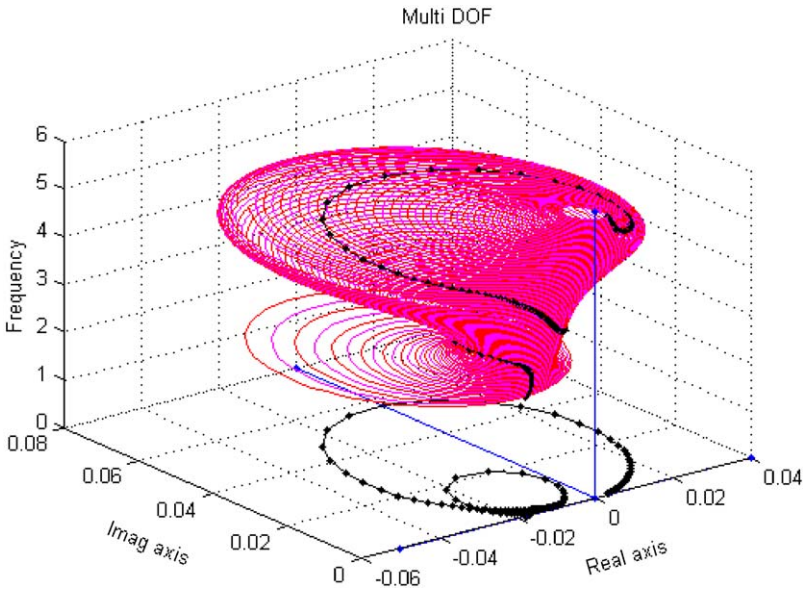

Fig. 2. Response as a function of stiffness and frequency variation for a multi-degree-of-freedom system.

The response obtained when varying two parameters independently can be visualized by superimposing multiple Vincent circles. By covering all possible combinations of values for the two parameters, a feasible response region in the complex plane is formed, inside which the response must lie.

The boundary of the feasible response region is obtained when the Jacobian of the transformation $a(z_1, z_2) = a_r(z_1, z_2) + \mathrm{i}a_i(z_1, z_2)$ becomes zero [3]:

$$\begin{vmatrix} \partial a_r/\partial z_1 & \partial a_r/\partial z_2 \\ \partial a_i/\partial z_1 & \partial a_i/\partial z_2 \end{vmatrix} = 0 \tag{20}$$

or, alternatively,

$$\mathrm{Im}\left(\frac{\partial a}{\partial z_1} \quad \frac{\partial a^*}{\partial z_2} \right) = 0, \tag{21}$$

when the two parameters z_1, z_2 are varied. The theoretical solution leads to a complicated formulation and consequently a numerical method is developed to obtain the boundary while avoiding the need for symbolic calculations.

Considering the response $a(z_1, z_2)$ and developing the perturbed response $a(z_1 + \Delta z_1,\ z_2 + \Delta z_2)$ as a first-order Taylor expansion

$$\begin{aligned} a(z_1 + \Delta z_1, z_2 + \Delta z_2) &= a(z_1, z_2) + \Delta z_1 \frac{\partial a}{\partial z_1} + \Delta z_2 \frac{\partial a}{\partial z_2} \\ &= a(z_1, z_2) + \begin{bmatrix} \dfrac{\partial a}{\partial z_1} & \dfrac{\partial a}{\partial z_2} \end{bmatrix} \begin{Bmatrix} \Delta z_1 \\ \Delta z_2 \end{Bmatrix} \\ &= a(z_1, z_2) + \begin{bmatrix} \dfrac{\partial a_r}{\partial z_1} + \mathrm{i}\dfrac{\partial a_i}{\partial z_1} & \dfrac{\partial a_r}{\partial z_2} + \mathrm{i}\dfrac{\partial a_i}{\partial z_2} \end{bmatrix} \begin{Bmatrix} \Delta z_1 \\ \Delta z_2 \end{Bmatrix} \\ &= a(z_1, z_2) + \begin{bmatrix} 1 & \mathrm{i} \end{bmatrix} \begin{bmatrix} \dfrac{\partial a_r}{\partial z_1} & \dfrac{\partial a_r}{\partial z_2} \\ \dfrac{\partial a_i}{\partial z_1} & \dfrac{\partial a_i}{\partial z_2} \end{bmatrix} \begin{Bmatrix} \Delta z_1 \\ \Delta z_2 \end{Bmatrix} \end{aligned} \tag{22}$$

which includes the Jacobian explicitly.

At a point of intersection $a(z_1, z_2) = a(z_1 + \Delta z_1, z_2 + \Delta z_2)$ it is seen that the matrix

$$\begin{bmatrix} \dfrac{\partial a_r}{\partial z_1} & \dfrac{\partial a_r}{\partial z_2} \\ \dfrac{\partial a_i}{\partial z_1} & \dfrac{\partial a_i}{\partial z_2} \end{bmatrix}$$

becomes singular for a particular increment in the modification, $\begin{Bmatrix} \Delta z_1 \\ \Delta z_2 \end{Bmatrix} \neq 0$. Thus, the locus of intersections at discrete intervals of the modification $\Delta z_1, \Delta z_2$ represents a close approximation to the boundary of the feasible region. In Fig. 3, C0 is the Vincent circle given when $z_1 \in C$ and $z_2 = 0$, and C1 and C2 are the two circles obtained when $z_2 \in C$ and z_1 takes fixed values separated by the small perturbation Δz_1. The intersection points between C1 and C2 determine the boundary of feasible modifications. In the particular case of Fig. 3 one of the intersections is very close to circle C0. This is because the increment Δz_1 separates two extremely close points on C0. The intersection does not lie on C0.

3. Numerical example

The example considered is the four-degree-of-freedom system, first described by Done and Hughes [2], shown in Fig. 4 with undamped natural frequencies of 1.05, 1.63, 2.48 and 4.99 rad/s. It can be observed that the oscillator m_4, k_5, c_3 acts as a damped vibration absorber on the rest of the system. We consider a series of

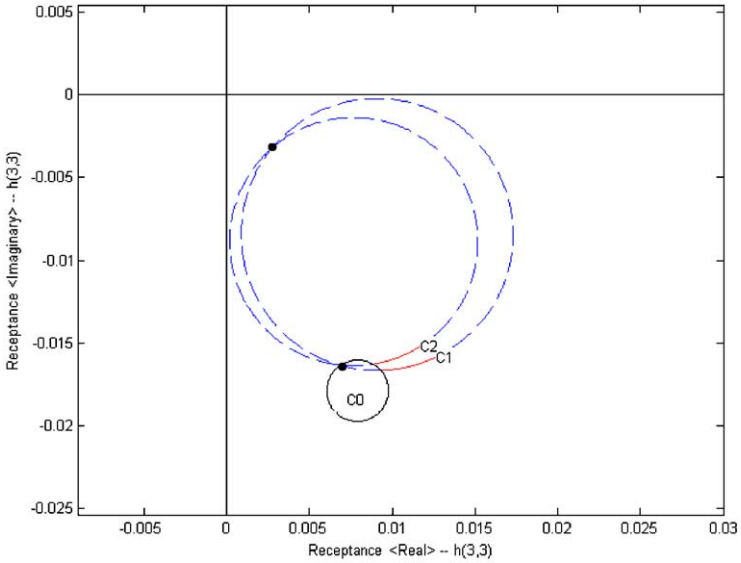

Fig. 3. Circle intersections defining the boundary of the feasible region.

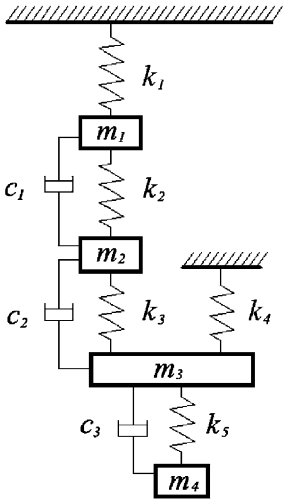

Fig. 4. Done and Hughes system: $k_1 = 40$, $k_2 = k_3 = k_4 = 30$, $m_1 = 3$, $m_2 = 10$, $m_3 = 20$, $m_4 = 5$, $c_1 = 0.5$, $c_2 = 0.6$, $c_3 = 0.8$.

applications to demonstrate how the Vincent circle method can be used in the analysis of vibration suppression problems.

3.1. The Vincent circle obtained by varying the stiffness of a spring

As a completely arbitrary first example we consider a modification by an added spring, Δk^*, connecting mass m_2 to ground and its affect upon the receptance h_{33}. When the modification takes values between $-\infty < \Delta k^* < \infty$ the circle representing the displacement response of the system at coordinate 3 to sinusoidal excitation at the same coordinate may be traced out as shown in Fig. 5. The centre of the circle is marked with '*', the point $\Delta k^* = 0$ with a small circle and the closest point to the origin with a black dot. The range

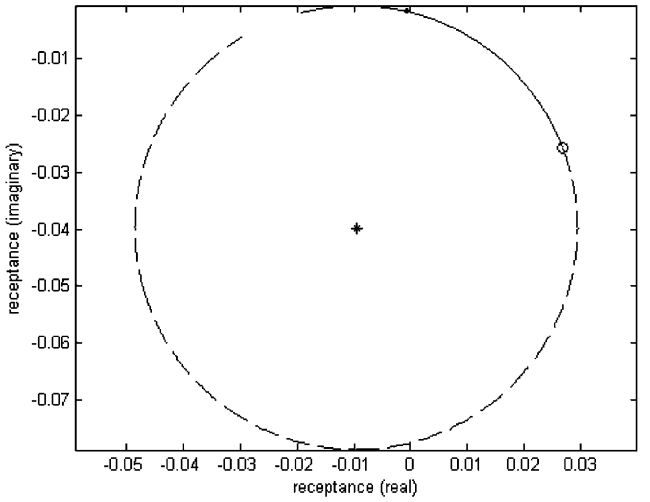

Fig. 5. The Vincent circle for receptance h_{33} with stiffness modification Δk_1.

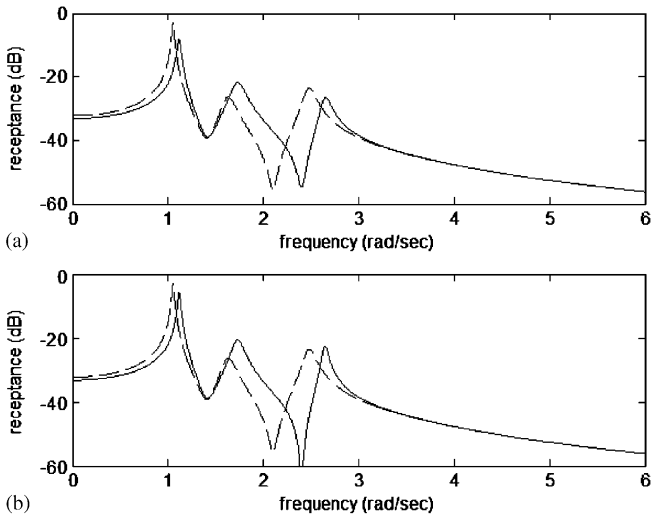

Fig. 6. Modified (full) and original receptances (dashed): (a) closest point on the circle and (b) exact assignment of the antiresonance.

$0<\Delta k^*<\infty$ is plotted as a full line and $-\infty<\Delta k^*<0$ as a dashed line. The example shown in the figure is for the excitation frequency of 2.4 rad/s. In vibration suppression problems the problem might be interpreted as finding the value of Δk^* corresponding to the point on the circle closest to the origin of the complex plane. A closed-form solution is described by Mottershead and Ram [7]. In the example the value of the modification at the closest point is $\Delta k^* = 14.78$ and the modification required to assign a antiresonance at exactly 2.4 rad/s is found [7] to be $\Delta z^* = 14.67 - 1.66\mathrm{i}$, so that in the latter case modifications to both stiffness and damping are necessary. Fig. 6 shows the original and modified receptances for the two cases (a) the closest strictly real modification $\Delta k^* = 14.78$ and (b) the exact assignment of the antiresonance $\Delta z^* = 14.67 - 1.66\mathrm{i}$.

Next consider modification of the fifth spring. Fig. 7 shows two Vincent circles produced when $\omega = 1.5$ rad/s corresponding to $c_3 = 0.8$ and 0. The smaller of the two circles is the damped one and it can be observed immediately that the larger circle passes exactly through zero when $k_5 + \Delta k_5 = \omega^2 m_4 = 11.25$, which is as expected the exact assignment of an antiresonance for the undamped absorber. The point on the damped-absorber circle closest to the origin is at $\Delta k_5 = 1.61$.

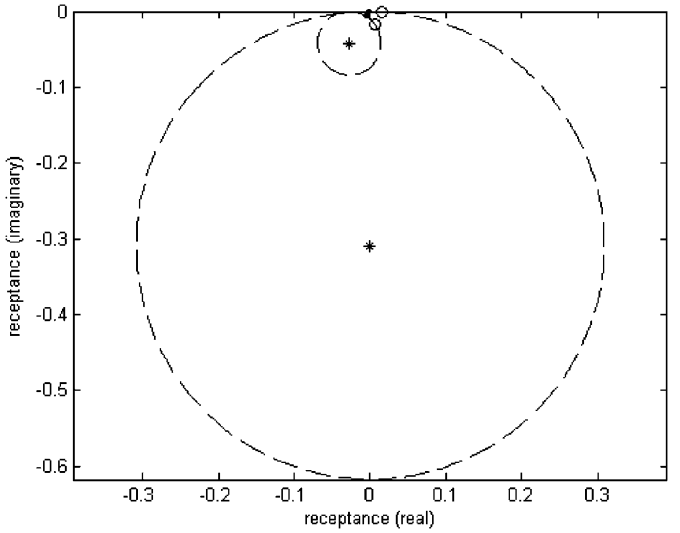

Fig. 7. Vincent circle for receptance h_{33} with stiffness modification Δk_5.

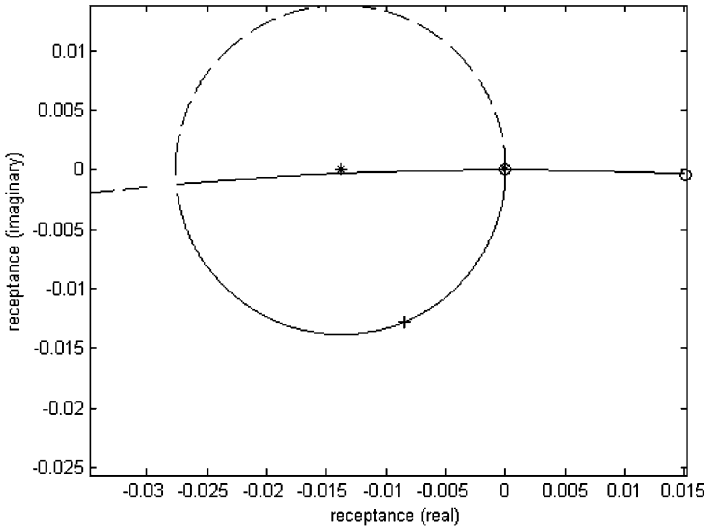

Fig. 8. Vincent circle with damping modification Δc_3.

3.2. The Vincent circle obtained by varying a damping coefficient

Fig. 8 shows the Vincent circle of parameter Δc_3 superimposed on part of the larger Vincent circle in Fig. 7. The large Vincent circle is for $-\infty < \Delta k_5 < 0$ while $k_5 = 10$ and $c_3 = 0$ and the other, smaller, Vincent circle is for $-\infty < \Delta c_3 < 0$ while $k_5 = 11.25$ and $c_3 = 0$. This value of k_5 is the one that exactly assigns an antiresonance when $c_3 = 0$ and therefore the small circle at the intersection, when $c_3 = 0$, is also at the origin of the complex plane of the receptance h_{33}. The small '+' sign denotes $c_3 = 1.6$, twice the value used by Done and Hughes [3]. It is clear that the distance of the '+' from the origin remains small, but the bandwidth of the antiresonance is considerably improved as shown in Fig. 9. Apparently the first mode is not affected very much by the absorber damper but the second node is very considerably diminished. If the mass m_4 is increased then the first mode is moved to the left, which may further increase the bandwidth. In the case of $m_4 = 20$ it is necessary to make a

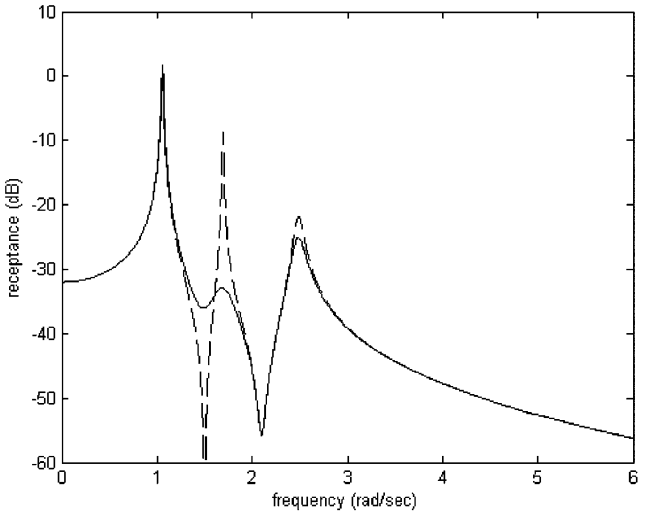

Fig. 9. Receptance h_{33} when $c_3 = 1.6$.

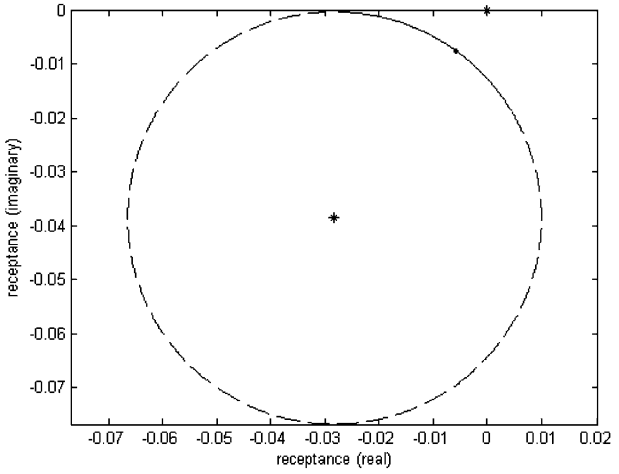

Fig. 10. Vincent circle h_{33} for $c_3 = \alpha k_5 + \beta$.

stiffness modification $k_5 = 35$ in order to maintain the antiresonance at 1.5 rad/s, but a considerable further increase in bandwidth is achieved.

3.3. *Vincent circle obtained by varying stiffness and damping together* ($c_3 = \alpha k_5 + \beta$)

The most general case of a stiffness and damping modification in the form $c_3 = \alpha k_5 + \beta$ is now considered. In our case we consider $\alpha = 0.01$, $\beta = 0.1$. The closest point to the origin is found to be at $k_5 = 1.69$ as shown in Fig. 10.

3.4. *Multiple circles obtained by varying two parameters independently*

The Vincent circle method is readily extended to the case of two independently varied parameters. The circles of the second parameter are then superimposed on the single circle of the first parameter, each second–parameter circle corresponding to a constant value of the first parameter. In Fig. 11 the two

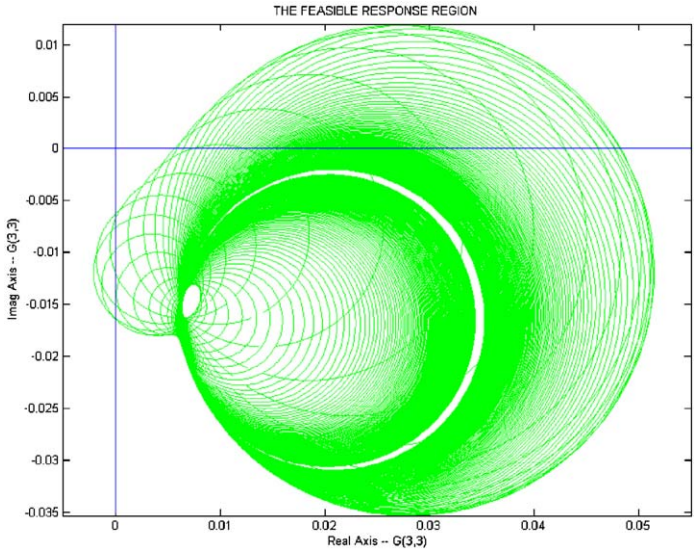

Fig. 11. Vincent circles h_{33} when $-\infty < k_3 < \infty$, $-\infty < k_5 < \infty$.

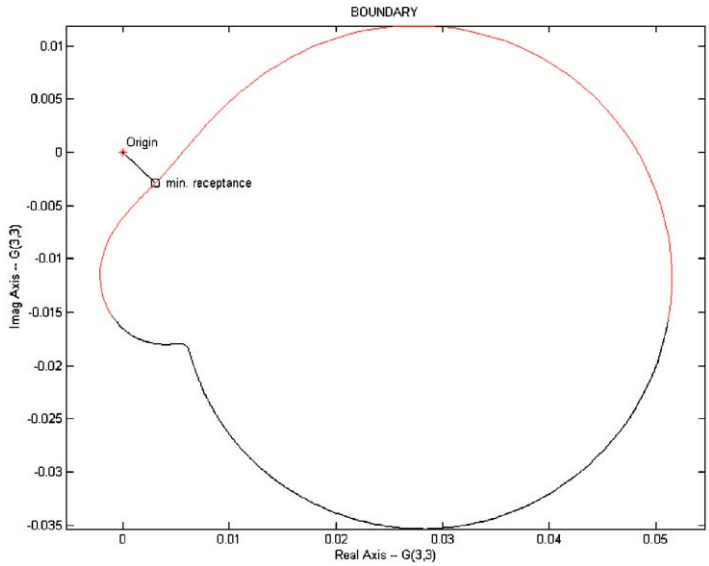

Fig. 12. Boundary of the superimposed Vincent circles.

parameters are k_3 and k_5. The circles of the second parameter, k_5, are each plotted for a constant value k_3 incremented between $-\infty$ and $+\infty$. Then at each constant value of k_3 a circle is traced when $-\infty < k_5 < \infty$. The boundary of the region encompassed by the circles is shown in Fig. 12 together with the vector to the closest point, which corresponds in this case to $k_3 = -23.23$, $k_5 = -2.4$.

4. Experimental examples

Experiments were carried out on a steel beam with the length of 1.6 m having a rectangular cross-section with nominal dimensions of 2 cm breadth by 1 cm depth in free–free and free–clamped (cantilever)

configurations. The beam was described by using 17 coordinates at equal spacings of 0.1 m along the beam. Antiresonances were assigned by added masses having magnitudes determined from Vincent's circles.

4.1. Free-free beam

In this experiment a minimum was assigned to receptance $h_{13,13}$ at 500 rad/s at coordinate 13, located 1.2 m from coordinate 1 at one end of the beam. A sixth-order polynomial was fitted to the measured receptances over a range from 350–600 rad/s, which resulted in the following measurements at 500 rad/s.

$$h_{13,13} = -4.3591 \times 10^{-6} - \mathrm{i} \times 2.3622 \times 10^{-7},$$
$$h_{1,13} = -9.4057 \times 10^{-6} - \mathrm{i} \times 2.7544 \times 10^{-7},$$
$$h_{13,1} = -9.6292 \times 10^{-6} - \mathrm{i} \times 4.1856 \times 10^{-7},$$
$$h_{1,1} = -1.7089\mathrm{e} \times 10^{-5} - \mathrm{i} \times 1.5972 \times 10^{-7}.$$

Application of Vincent's circle resulted in a mass modification of 1.09 kg at coordinate 1. The complete circle is shown in Fig. 13(a), where it is seen that the range of positive mass modifications (given by the full line) is very small and the negative solutions extend to almost the entire circumference. The close-up view, in Fig. 13(b), shows that there is indeed a positive mass solution. Fig. 14 shows the original receptance $h_{13,13}$ (full line) and the same receptance after physical application of the mass modification (dashed line). It can be seen

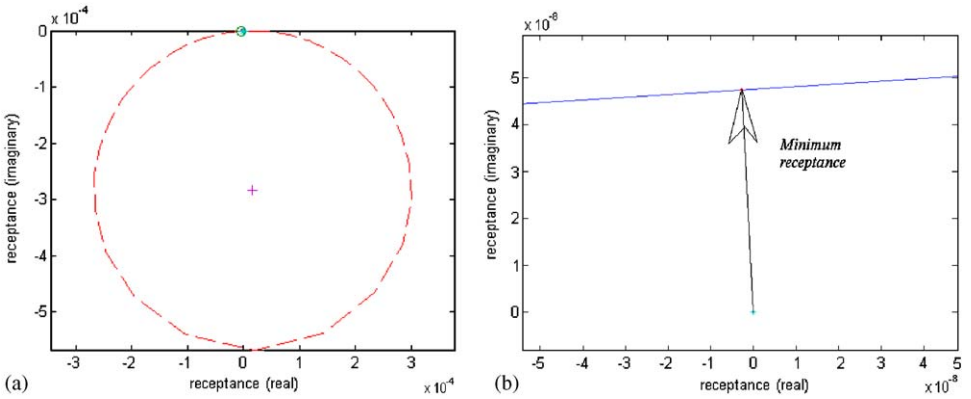

Fig. 13. Vincent's circle for the first free–free experiment: (a) complete circle and (b) zoom plot showing the point of minimum receptance.

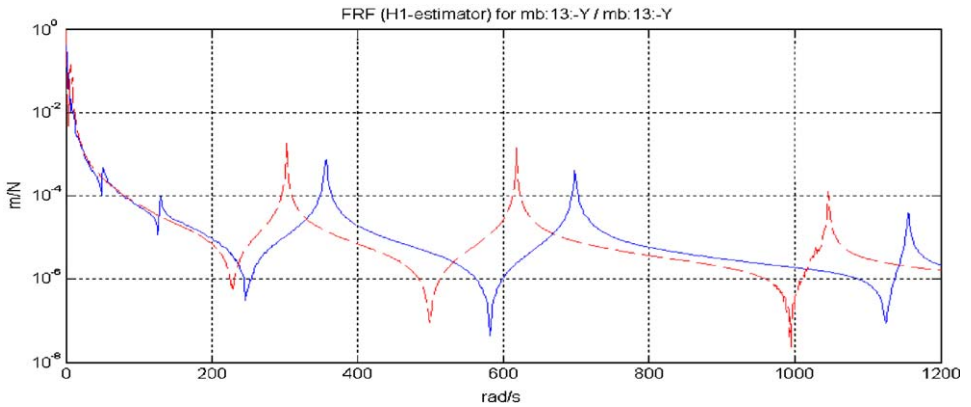

Fig. 14. Measured receptances $h_{13,13}$ from the free–free beam: full line: before modification and dashed line: after modification.

that the zero around 590 rad/s in the original system is relocated to a point very close to 500 rad/s by the added mass.

In a second experiment using the free–free configuration a zero of $h_{17,13}$ was assigned to 450 rad/s by means of a mass modification of 0.165 kg at coordinate 1. The following measurements were obtained from smoothed data at 450 rad/s:

$$h_{13,13} = 3.9999 \times 10^{-6} - \mathrm{i} \times 6.9564 \times 10^{-7},$$
$$h_{1,13} = 1.7699 \times 10^{-5} - \mathrm{i} \times 1.0382 \times 10^{-6},$$
$$h_{13,1} = -1.3356 \times 10^{-5} - \mathrm{i} \times 2.7977 \times 10^{-7},$$
$$h_{1,1} = -2.8561 \times 10^{-5} - \mathrm{i} \times 1.3138 \times 10^{-6}.$$

The Vincent circle is shown in Fig. 15, and Fig. 16 shows the original (full line) and modified (dashed line) receptance $h_{17,13}$. It can be seen that the zero around 500 rad/s in the original system is relocated to a point very close to the target frequency of 450 rad/s in the modified system.

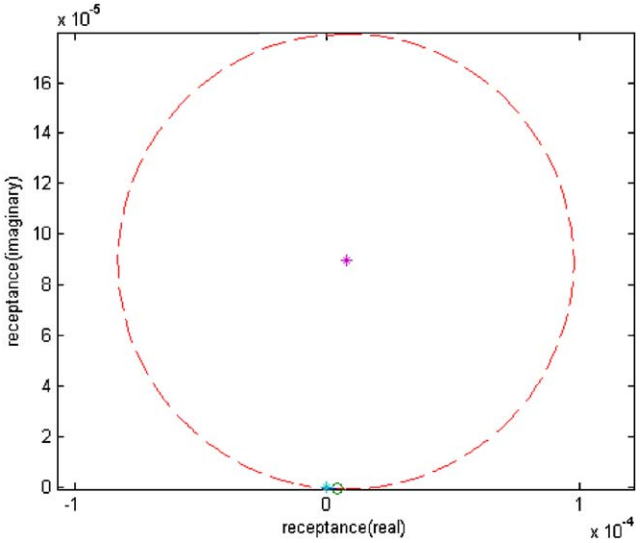

Fig. 15. Vincent circle for the second free–free experiment.

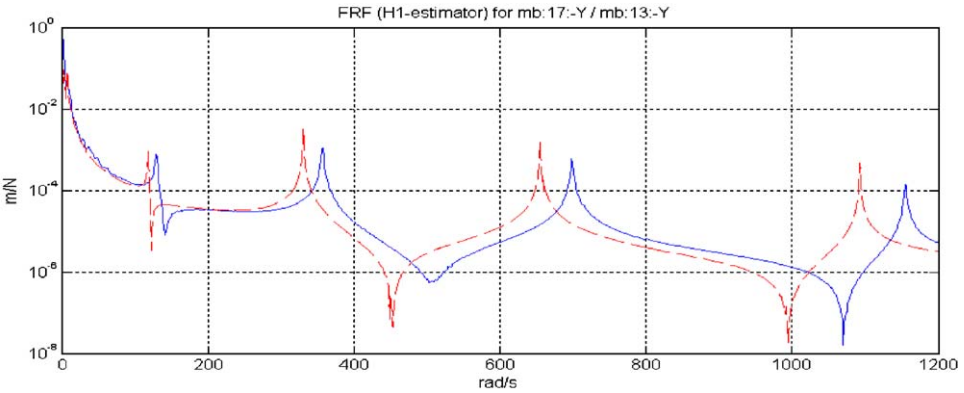

Fig. 16. Measured receptances $h_{17,13}$ from the free–free beam: full line: before modification and dashed line: after modification.

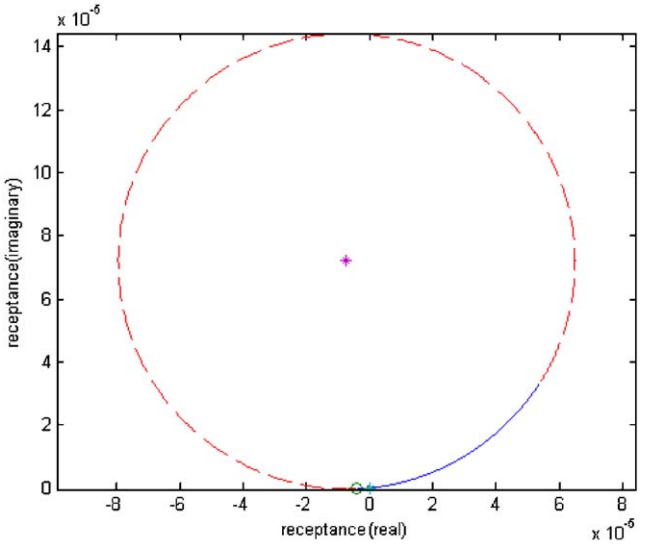

Fig. 17. Vincent's circle for the clamped–free experiment.

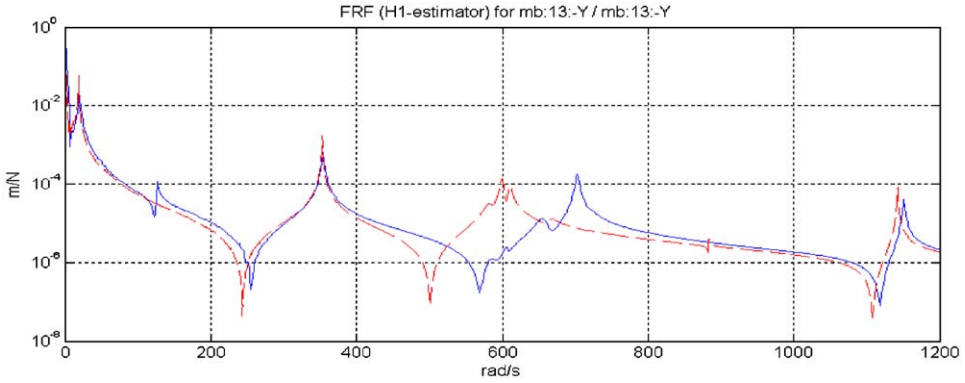

Fig. 18. Measured receptances $h_{13,13}$ from the clamped–free beam: full line: before modification and dashed line: after modification.

4.2. Clamped–free beam

A zero of $h_{13,13}$ was assigned to 500 rad/s by means of a mass modification of 0.62 kg at coordinate 9 (at midspan). The following smoothed measurements were obtained at 500 rad/s:

$$h_{9,9} = -3.9948 \times 10^{-6} - \mathrm{i} \times 2.2412 \times 10^{-7},$$
$$h_{9,13} = -5.2125 \times 10^{-6} - \mathrm{i} \times 1.1579 \times 10^{-7},$$
$$h_{13,9} = -5.2463 \times 10^{-6} - \mathrm{i} \times 1.2293 \times 10^{-7},$$
$$h_{13,13} = -3.6081 \times 10^{-7} + \mathrm{i} \times 1.8944 \times 10^{-7}.$$

The Vincent circle is shown in Fig. 17 where it can be seen the arc of positive mass modification is much greater than in the previous two examples. Fig. 18 shows the original (solid line) and modified (dashed line) receptance $h_{13,13}$ and similarly to the previous examples it can be seen that the zero around 580 rad/s in the original system is relocated to a point very close to 500 rad/s for the modified system.

5. Conclusions

The Vincent circle is generalized to include the case of a straight line modification $c = \alpha(k - \omega^2 m) + \beta$ and is shown to be a special case of the bilinear transformation due to Moebius. A new method is presented for the visualization of Vincent circle results, especially when more than one modification is considered. The method is demonstrated in simulations and physical experiments. In the former, damping and general straight-line modifications are considered. In the latter, the zeros of point and cross receptances are assigned by adding point masses to a beam.

Acknowledgement

The research described in this paper was supported in part by EPSRC Grant GR/R43563.

Appendix A. Derivation of the Vincent circle for the general straight-line modification $z = k + \mathrm{i}\omega c - \omega^2 m$, where $c = \alpha(k - \omega^2 m) + \beta$

It is required to find the nature of the complex equation (8) for the general modification $z = k + \mathrm{i}\omega c - \omega^2 m$, where $c = \alpha(k - \omega^2 m) + \beta$.

Let $a = p + \mathrm{i}q$, $b = r + \mathrm{i}s$, $c = t + \mathrm{i}u$ and $d = v + \mathrm{i}w$.

Substituting $z = (k - \omega^2 m)(1 + \mathrm{i}\alpha\omega) + \mathrm{i}\beta\omega$ in Eq. (8) yields

$$p + \mathrm{i}q = r + \mathrm{i}s + \frac{\big[\big((k - \omega^2 m) + \mathrm{i}\alpha\omega(k - \omega^2 m)\big) + \mathrm{i}\beta\omega\big](t + \mathrm{i}u)}{1 + [((k - \omega^2 m) + \mathrm{i}\alpha\omega(k - \omega^2 m)) + \mathrm{i}\beta\omega](v + \mathrm{i}w)}. \tag{A.1}$$

Simplifying Eq. (A.1)

$$\begin{aligned}&(p - r) + \mathrm{i}(q - s)\\ &\quad = \frac{t\big((k - \omega^2 m) + \mathrm{i}\alpha\omega(k - \omega^2 m)\big) + \mathrm{i}u\big((k - \omega^2 m) + \mathrm{i}\alpha\omega(k - \omega^2 m)\big) + \mathrm{i}t\beta\omega - u\beta\omega}{1 + v((k - \omega^2 m) + \mathrm{i}\alpha\omega(k - \omega^2 m)) + \mathrm{i}w((k - \omega^2 m) + \mathrm{i}\alpha\omega(k - \omega^2 m)) + \mathrm{i}v\beta\omega - w\beta\omega}.\end{aligned} \tag{A.2}$$

Eq. (A.2) can be written as

$$\begin{aligned}&[(p - r) + \mathrm{i}(q - s)]\big[1 + v\big((k - \omega^2 m) + \mathrm{i}\alpha\omega(k - \omega^2 m)\big) + \mathrm{i}w\big((k - \omega^2 m) + \mathrm{i}\alpha\omega(k - \omega^2 m)\big) + \mathrm{i}v\beta\omega - w\beta\omega\big]\\ &\quad = \big[t\big((k - \omega^2 m) + \mathrm{i}\alpha\omega(k - \omega^2 m)\big) + \mathrm{i}u\big((k - \omega^2 m) + \mathrm{i}\alpha\omega(k - \omega^2 m)\big) + \mathrm{i}t\beta\omega - u\beta\omega\big].\end{aligned} \tag{A.3}$$

The real part of Eq. (A.3) gives

$$\begin{aligned}&[(p - r) - (p - r)w\beta\omega - (q - s)v\beta\omega + u\beta\omega]\\ &\quad = (k - \omega^2 m)[t - u\alpha\omega + (q - s)d + (q - s)v\alpha\omega + (p - r)w\alpha\omega - (p - r)v]\end{aligned} \tag{A.4}$$

and the imaginary part of Eq. (A.3) yields

$$\begin{aligned}&[(q - s) + (p - r)v\beta\omega - (q - s)w\beta\omega - t\beta\omega]\\ &\quad = (k - \omega^2 m)[u + t\alpha\omega - (p - r)d + (p - r)v\alpha\omega + (q - s)w\alpha\omega - (q - s)v].\end{aligned} \tag{A.5}$$

Dividing Eqs. (A.4) by (A.5) results in deleting the modification term $(k - \omega^2 m)$,

$$\begin{aligned}&\frac{(p - r) - (p - r)w\beta\omega - (q - s)v\beta\omega + u\beta\omega}{(q - s) - (q - s)w\beta\omega + (p - r)v\beta\omega - t\beta\omega}\\ &\quad = \frac{t - u\alpha\omega + (q - s)w + (q - s)v\alpha\omega + (p - r)w\alpha\omega - (p - r)v}{u + t\alpha\omega - (p - r)w + (p - r)v\alpha\omega + (q - s)w\alpha\omega - (q - s)v}.\end{aligned} \tag{A.6}$$

Vincent's circle is derived by rearranging Eq. (A.6)

$$(p-r)^2+(q-s)^2+\frac{-u-t\alpha\omega+2\beta\omega(uw+tv)}{w+v\alpha\omega-\beta\omega(v^2+w^2)}(p-r)+\frac{t-u\alpha\omega+2\beta\omega(uv-tw)}{w+v\alpha\omega-\beta\omega(v^2+w^2)}(q-s)$$
$$=\frac{\beta\omega(t^2+u^2)}{w+v\alpha\omega-\beta\omega(v^2+w^2)}. \tag{A.7}$$

To define the centre and radius of the circle, Eq. (A.7) is written in the form of the standard circle equation

$$\left[p-\left(r+\frac{u+t\alpha\omega-2\beta\omega(uw+tv)}{2(w+v\alpha\omega-\beta\omega(v^2+w^2))}\right)\right]^2+\left[q-\left(s+\frac{-t+u\alpha\omega-2\beta\omega(uw-tw)}{2(w+v\alpha\omega-\beta\omega(v^2+w^2))}\right)\right]^2$$
$$=\frac{4\beta\omega(t^2+u^2)\left[w+v\alpha\omega-\beta\omega(v^2+w^2)\right]+[u+t\alpha\omega-2\beta\omega(uw+tv)]^2+[-t+u\alpha\omega-2\beta\omega(uv-tw)]^2}{4(w+v\alpha\omega-\beta\omega(v^2+w^2))^2}. \tag{A.8}$$

Let

$$A=w+v\alpha\omega-\beta\omega(v^2+w^2) \tag{A.9}$$

and write

$$t^2+u^2=cc^*,\ v^2+w^2=dd^*. \tag{A.10}$$

Then the radius of the circle is given from the left-hand side of Eq. (A.8). After expanding the two squared terms in the numerator and simplifying it is found that,

$$\rho^2=\frac{\beta\omega cc^*}{A}+\frac{cc^*(1+\alpha^2\omega^2-4\alpha\beta\omega^2w-4\beta\omega v+4\beta\omega^2dd^*)}{4A^2} \tag{A.11}$$

or after further simplification

$$\rho=\sqrt{\frac{\beta\omega cc^*}{A}+BB^*}, \tag{A.12}$$

where

$$B=\frac{\omega((\alpha-2\beta d^*)-\mathrm{i})c}{2A}\ \text{and}\ B^*=\frac{\omega((\alpha-2\beta d^*)+\mathrm{i})c^*}{2A}. \tag{A.13}$$

The centre of the circle can be expressed as

$$\xi=b+B. \tag{A.14}$$

References

[1] A.H. Vincent, A note on the properties of the variation of structural response with respect to a single structural parameter when plotted in the complex plane, Westland Helicopters Ltd., Report GEN/DYN/RES/010R, September 1973.

[2] H. Schwerdtfeger, *Geometry of Complex Numbers—Circle Geometry, Moebius Transformation, Non-Euclidian Geometry*, Dover Publications, New York, 1979.

[3] G.T.S. Done, A.D. Hughes, The response of a vibrating structure as a function of structural parameters, *Journal of Sound and Vibration* 38 (2) (1975) 255–266.

[4] E.J. Nagy, Vincent's circle as a tool for machine vibration optimisation techniques, ASME paper 81-DET-78.

[5] H.W. Hanson, N.J. Calapodas, Evaluation of the practical aspects of vibration reduction using structural optimisation techniques, *Journal of the American Helicopter Society* 25 (3) (1980) 37–45.

[6] J.E. Mottershead, Structural modification for the assignment of zeros using measured receptances, *Transactions of the American Society of Mechanical Engineers, Journal of Applied Mechanics* 68 (5) (2001) 791–798.

[7] J.E. Mottershead, Y.M. Ram, Inverse eigenvalue problems in vibration absorption: passive modification and active control, *Mechanical Systems and Signal Processing,* in press.

[8] G.H. Golub, C.F. Van Loan, *Matrix Computations*, second ed., The John Hopkins University Press, Baltimore, London, 1989.